

## **Sound induces change in orientation preference of V1 neurons: Audio-visual cross-influence**

*Nayan Chanauria<sup>1</sup>, Vishal Bharmauria<sup>2</sup>, Lyes Bachatene<sup>3</sup>, Sarah Cattan<sup>4</sup>, Jean Rouat<sup>1, 5</sup>, Stéphane Molotchnikoff<sup>1, 5</sup>*

<sup>1</sup>Neurophysiology of Visual System, Département de Sciences Biologiques, Université de (Kayser & Logothetis, 2007)Montréal, CP 6128 Succursale Centre-Ville, Montréal, QC H3C 3J7, Canada

<sup>2</sup>The Visuomotor Neuroscience Lab, Centre for Vision Research, Faculty of Health, York University, Toronto, ON, Canada

<sup>3</sup>Department of Nuclear Medicine and Radiobiology, Faculty of Medicine and Health Sciences (CHUS), SNAIL, Sherbrooke Neuro Analysis and Imaging Lab, University of Sherbrooke, Sherbrooke, QC, Canada

<sup>4</sup>Institut de Neurosciences de la Timone, Faculté de Médecine, 27, Boulevard Jean Moulin 13005 Marseille, France

<sup>5</sup>Département de Génie Électrique et Génie Informatique, Université de Sherbrooke, Sherbrooke, QC, Canada

**Keywords:** plasticity, primary visual cortex, infragranular, supragranular, non-visual input, sound repetition, orientation selectivity, cross-modal, audio-visual, supramodal, multisensory integration

## **Abstract**

In the cortex, demarcated unimodal sensory regions often respond to unforeseen sensory stimuli and exhibit plasticity. The current investigation aimed to test responses of primary visual cortex (V1) neurons in response to an adapting auditory stimulus by entirely refraining visual stimulus during sound stimulation. Using extracellular recordings in anesthetized cats, we demonstrate that, unlike the prevailing observation of only a slight modulation in the firing rate of the neurons, sound imposition entirely shifted the orientation selectivity of visual neurons in both supra- and infragranular layers of V1. Our results suggest that neurons specific to either layer dynamically integrate features of the sound and change the V1 organization. Intriguingly, these experiments present novel findings that the mere presentation of a prolonged auditory stimulus may drastically recalibrate the tuning properties of visual neurons. These results highlight the phenomenal neuroplasticity of visual neurons and certainly initiate a new line of research in cross-modal plasticity.

## Introduction

In spite of the fact that inputs to a primary sensory area have been thought to be largely modality specific, a emerging notion proposes a direct and more specific interaction between the early sensory cortices of different modalities (Kayser & Logothetis, 2007). Per se, regions like primary visual cortex (V1) are conservative and considered to be excited exclusively by visual input. Multimodal research has steered a new insight into the brain organization and perception. Several studies have suggested that the meeting and interaction of information from different senses initiate within the low-level sensory areas (Ghazanfar & Schroeder, 2006; van Atteveldt *et al.*, 2014; Ten Oever *et al.*, 2015). Further, more findings propose that even low-order sensory areas may contribute to multisensory processing starting from a very early stage (Schroeder *et al.*, 2003; Foxe & Schroeder, 2005; Macaluso & Driver, 2005). Some fMRI studies also support this line of thought (Clavagnier *et al.*, 2004; Kayser *et al.*, 2005). Moreover, studies in non-human primates have revealed direct cortico-cortical pathways from primary auditory (A1) to primary visual cortex (V1) (Rockland & Van Hoesen, 1994; Falchier *et al.*, 2002; Rockland & Ojima, 2003; Clavagnier *et al.*, 2004; Budinger *et al.*, 2006). Direct anatomical connections from V1 to A1 are not precisely known, but it is known that visual area V2 is directly connected with A1 (Budinger *et al.*, 2006). An alternative yet slightly longer pathway between A1 and V1 through the heteromodal association cortical area was also thought to send feedback to both A1 and V1. This area comprised of the superior temporal polysensory area and superior temporal sulcus (STP/STS) (Schroeder & Foxe, 2002). A critical study (Liang *et al.*, 2013) revealed that there might be salient locations within the V1 that respond to specific cross-modal inputs related to the spatial pattern of activation of a primary sensory cortical area (e.g., V1) and input stimuli from a different modality (e.g., audio or tactile). In humans, it has been shown that reaction-time speeds up when sensory information from different modalities are combined (Hershenson, 1962; Gielen *et al.*, 1983). Two recent cases enabled to understand different facets of cross-modal processing. Ibrahim and co-authors (Ibrahim *et al.*, 2016) demonstrated sharpening of orientation tuning in conjunction with an enhancement of the response to the preferred orientation of the cell, predominantly when a low-contrast visual stimulus was accompanying an auditory stimulus. On the contrary, Iurilli and colleagues (Iurilli *et al.*, 2012) revealed that presentation of a high-amplitude sound stimulus resulted in the hyperpolarization of the membrane potential of V1 neurons resulting in inhibition. From all of the above, it appears that V1 neurons adopt a different outline of processing towards the multimodal configuration of stimulus features.

Despite extensive experimentation to explore multimodal interactions in the cortex, the role of cross-modal inputs in modulating sensory processing features of cortical neurons and the precise underlying mechanism remain unstated. To date, most studies have limited the presentation of stimuli for a very short

duration. Additionally, mostly rodents have been the first choice for electrophysiological experimentation in this direction and imaging is being fully exploited in humans. In the present investigation, a sound stimulus was applied to V1 neurons in cats in the complete absence of a visual input for 12 minutes. To this goal, through extracellular recordings in area 17 of anesthetized cats, we found that in the presence of a non-visual input, in our case a sound stimulus, the orientation tunings of simultaneously recorded layer 2/3 and layer 5/6 visual neurons were fully altered, while exhibiting shifts in their tuning. Also, the orientation shift magnitude was found to be larger in layer 5/6 neurons. We argue and suggest that the modification was solely potentiated by the continuous repetition of the sound stimulus for 12 min and the spatial-temporal structure of the sound. Interestingly, layer 2/3 neurons displayed an intriguing shift pattern towards horizontal orientations unlike layer 5/6. Our data illustrate a novel extension to audio-visual cross-influence demonstrating that even an isolated application of a sound can robustly induce a reorganization of area V1. Our data exemplifies supramodal nature and cross-modal interactions in the V1 that possibly occur early during a multisensory integration process in response to a sensory stimulus that differs in its expected matching response region. While we are too far to certify that the whole neocortex is multisensory in function, conclusions from a variety of protocols may give better insights into multisensory integration in the cortex.

## **Materials and methods**

### **Ethical approval**

Eight adult domestic cats (*Felis catus*) of either sex were used for experiments adhering to the guidelines approved by the NIH in the USA and the Canadian Council on Animal Care. Cats were supplied by the Division of Animal Resources of the University of Montreal. The animal surgery and electrophysiological recording procedures were performed according to the guidelines of the Canadian Council on Animal Care and were approved by the Institutional Animal Care and Use Committee of the University of Montreal (CDEA).

### **Anesthesia**

Cats were initially sedated with a mixture of Atravet (0.1 mg/kg, s.c., Wyeth-Ayerst, Guelph, ON, Canada) and atropine sulphate (0.04 mg/kg, s.c., Atrosa; Rafter, Calgary, AB, Canada) followed by a dose of anesthetic ketamine (40 mg/kg, i.m., Narketan; Vetoquinol, QC, Canada). Anesthesia was maintained during the surgery with isoflurane ventilation (2%, AErrane; Baxter, Toronto, ON, Canada). After the surgery, cats were fixed on the stereotaxic and were paralyzed by perfusion of gallamine triethiodide (40 mg/kg, i.v., Flaxedil; Sigma Chemical, St Louis, MO, USA). Artificial ventilation was maintained by a mixture of O<sub>2</sub>/N<sub>2</sub>O (30: 70) and isoflurane (0.5%). The paralysis was continued by perfusion of gallamine

triethiodide (10 mg/kg/h) in 5% dextrose lactated Ringer's nutritive solution (i.v., Baxter, Mississauga, ON, Canada) throughout the experiment.

### **Surgery**

Local anesthetic xylocaine (2%; AstraZeneca, Mississauga, ON, Canada) was injected subcutaneously during the surgery before any opening of the skin. A heated pad was placed beneath the cat to maintain a body temperature of 37.5 °C. Antibiotics Tribissen (30 mg/kg/day, subcutaneous; Schering Plough, Pointe-Claire, QC, Canada) and Duplocillin (0.1 mL/kg, intra-muscular; Intervet, Withby, ON, Canada) were administered to the animals to prevent bacterial infection. First, a vein of the animal's forelimb was cannulated. Then tracheotomy was performed to artificially ventilate the animal. A proper depth of anesthesia was ensured throughout the experiment by monitoring the EEG, the electrocardiogram, and the expired CO<sub>2</sub>. O<sub>2</sub> saturation was kept in check using an Oximeter. The end-tidal CO<sub>2</sub> partial pressure was kept constant between 25 and 30 mmHg. Third, craniotomy (1\*1 cm) was performed over the primary visual cortex (area 17/18, Horsley-Clarke coordinates P0-P6; L0-L6). The underlying dura was removed, and the depth electrode was positioned in area 17. The pupils were dilated with atropine sulfate (1%; Isopto-Atropine, Alcon, Mississauga, ON, Canada) and the nictitating membranes were retracted with phenylephrine hydrochloride (2.5%; Mydrin, Alcon). Plano contact lenses with artificial pupils (5 mm diameter) were placed on the cat's eyes to prevent the cornea from drying. Finally, the cats were sacrificed with a lethal dose of pentobarbital sodium (100 mg/kg; Somnotol, MTC Pharmaceuticals, Cambridge, ON, Canada) by an intravenous injection.

### **Stimuli and experimental design**

Two types of stimuli were used in the experiments- visual and audio. First, the receptive fields were located centrally within a 15° radius from the fovea. Monocular stimulation was performed. Receptive field edges (RF) were explored once clear detectable activity was obtained using a handheld ophthalmoscope (Barlow *et al.*, 1967). This was done by moving a light bar from the periphery toward the center until a response was evoked. Contrast and mean luminance was set at 80% and 40cd/m<sup>2</sup>, respectively. Optimal spatial and temporal frequencies were set at 0.24 cycles/deg and in the range 1.0–2.0 Hz (at these values V1 neurons are driven maximally) for drifting sine-wave gratings (Bardy *et al.*, 2006). Then, gratings were presented randomly as visual stimuli covering the excitatory RF to compute the orientation tuning curves of neurons (Maffei *et al.*, 1973). Visual stimuli were generated with a VSG 2/5 graphics board (Cambridge Research Systems, Rochester, England) and displayed on a 21-inch Monitor (Sony GDM-F520 Trinitron, Tokyo, Japan) placed 57 cm from the cat's eyes, with 1024×9×768 pixels, running at 100 Hz frame refresh (Figure 1 A). The gratings moved unidirectionally in eight possible

orientations presented randomly one by one. Each randomly presented oriented grating was given 25 times for 4s each with an inter-stimulus interval of 1-3s. Subsequently, the animal was exposed to broadband noise-like auditory stimuli comprising a range of frequencies. The auditory stimulus (3s 78 dB SPL) consisted of temporally orthogonal rippled combinations (TORC's) with varying frequency components from 250 Hz to 8000 Hz (Fries *et al.*, 2007). The 3s stimulus was played continuously for 12 minutes, was delivered by a pair of external loudspeakers (120 Hz-18 KHz) and positioned perpendicularly relative to the animal axis at 57 cm to the center of the fixation axis of the animal. For some recordings, the speakers were also displaced laterally at the same plane, at 30 cm on either side from the center of the fixation axis of the cat. This was done to test the difference in responses when the position of speakers was changed. The sound frequency and intensity were cyclical and optimized and set according to the experiment design using Bruel and Kjaer Spectris Group Sonometer. The stimulus was optimized on a standard C-scale of the sonometer for both ears. The spectrogram of the sound stimulus displaying varying frequencies is shown in Figure 1 B. After the 12-min presentation of the acoustic stimulus, a series of drifting gratings was presented again in a random order (each oriented grating presented 25 times, 4s each and inter-stimulus time interval). It must be emphasized that sound was applied in isolation, that is, no visual stimulus was presented during the sound application. Finally, a recovery period of 90 minutes was given for neurons to return to their optimal state (Figure 1 C).

### **Electrophysiology**

Multiunit activity in the primary visual cortex of anesthetized cats was recorded using a tungsten multichannel depth electrode (0.1–0.8 M $\Omega$  at 1 KHz; Alpha Omega Co. USA Inc). Neural activity was recorded from both hemispheres of the cat's brain. The depth electrode consisted of four microelectrodes enclosed in a stainless-steel tubing in a linear array with an inter-electrode spacing of 500  $\mu$ m. The recorded signal from the microelectrodes was acquired using Spike2, CED, Cambridge, UK. The signal was further amplified, band-pass filtered (300 Hz–3 KHz), digitized, displayed on an oscilloscope and recorded with a 0.05 ms temporal resolution. Recordings were performed at average cortical depths of 300–500  $\mu$ m and 1000–1200  $\mu$ m (Chanauria *et al.*, 2016) simultaneously from both sites as depicted in Figure 1 D. Spike sorting was done offline using same Spike2 package, CED, Cambridge, UK. Figure 2 shows an example of neuronal isolation (spike sorting) from the multiunit activity. As a precautionary measure, it was essential to affirm that we did not isolate the same unit twice, as the same unit may exhibit different waveforms depending upon several factors. Thus, the single units were discriminated based upon the spike waveforms, principal component analysis (PCA), and autocorrelograms (ACG) (Bharmauria *et al.*, 2015; Bharmauria *et al.*, 2016). The respective PCA, ACGs, and spike waveforms are also shown along in Figure 2.

## Data Analysis

### Tuning curves

After sorting neurons offline, the numerical value of orientation selectivity was calculated for each neuron at control and post-sound presentation conditions. The values were obtained by fitting a Gaussian non-linear curve on the raw orientation tuning values obtained at each orientation for each neuron. The Gaussian tuning fits were computed using the function below:

$$y = y_0 + \left( A \div \left( w \times \sqrt{\left( \frac{\pi}{2} \right)} \right) \right) \times e^{\left( -2 \times \left( \frac{x - XC}{w} \right)^2 \right)} \quad (\text{Equation 1})$$

where  $y_0$  is the offset,  $XC$  is the center,  $w$  is the width, and  $A$  represents the area under the Gaussian fit. The firing rates were normalized and gaussian tuning curves were generated in the scientific software Origin. The magnitude of shifts was computed as the distance (subtractions) between peak positions of the fitted Gaussian tuning curves before and after the presentation of sound (the difference between the initially preferred and newly acquired). The following formula was applied to calculate the shift magnitudes:

$$\text{Shift magnitude} = (XC_{\text{Post}} - XC_{\text{Pre}}) \quad (\text{Equation 2})$$

where  $XC$  is the central value derived from the Gaussian fit.

According to past studies, a difference of  $> 5^\circ$  is considered as a significant shift (Ghisovan *et al.*, 2009; Bachatene *et al.*, 2012a; Bachatene *et al.*, 2013; Bachatene *et al.*, 2015; Chanauria *et al.*, 2016). A magnitude of  $< 5^\circ$  indicated a neuron that retained its initially preferred orientation even after the presentation of sound. These calculations are critical as the interval of  $22^\circ$  between the stimulus orientations is relatively large, which makes it difficult to deduce an exact value of orientation tuning from only raw curves.

### Orientation Selectivity Index (OSI)

Further, the Orientation Selectivity Index (OSI) of each neuron was computed by dividing the firing rate of the neuron at the orthogonal orientation by the firing rate of the same neuron at the preferred orientation, and subtracting the result from 1 (Ramoia *et al.*, 2001; Liao *et al.*, 2004). The closer the OSI is to 1, the stronger the orientation selectivity.

$$\text{Orientation Selectivity Index} = 1 - (FR_{\text{Orthogonal}} / FR_{\text{Preferred}}) \quad (\text{Equation 3})$$

where FR is the firing rate of the same neuron.

### **Bandwidths (BW)**

Tuning bandwidths were calculated based on the full width at half magnitude (FWHM) of the Gaussian tuning curves for each neuron (Ringach *et al.*, 2002; Moore *et al.*, 2005). Bandwidths are measured to deduce the sharpness of orientation tuning curves of the neurons.

$$\text{FWHM (Bandwidth)} = 2 \sqrt{2 \ln 2} c = 2.35482c \quad (\text{Equation 4})$$

where  $\ln$  is the neperian logarithm and  $c$  is the gaussian root mean square width.

### **Response Change Index (RCI)**

To quantify the response disparity between stimulus conditions for each neuron, the traditional method of measuring response change index was used (Stevenson *et al.*, 2014; Meijer *et al.*, 2017) where the values of the RCI are normalized and can be used as a parameter to describe both enhancement and suppression. The values may range from -1 to 1 in which negative values indicate response suppression and positive values indicate response enhancement.

$$\text{RCI} = (\text{FR}_{\text{Postsound}} - \text{FR}_{\text{Control}}) / (\text{FR}_{\text{Postsound}} + \text{FR}_{\text{Control}}) \quad (\text{Equation 5})$$

where FR is firing rate of the same neuron

### **Statistical tests**

Five datasets from layer 2/3 and layer 5/6 were tested for statistics values of (i) orientation tunings of neurons (ii) amplitudes of shift; (iii) OSI of neurons at pre- and post-sound presentation conditions; and (iv) Bandwidth (v) Response Change Index. These data were tested for normal distribution using the Shapiro Wilk normality test. Based on the results obtained, parametric and non-parametric tests were applied on data sets. Consequently, comparisons were drawn between values of different parameters for either layer. Detailed information of tests can be found in legends of the figures as well as the results. The current investigation focused on how visual cells reacted towards oriented gratings when a sound stimulus was presented solely in the absence of any other visual stimulation. The extracellular activity of V1 neurons was simultaneously recorded from the layer 2/3 and 5/6 down the column. The gaussian tuning curves of neurons in layer 2/3 and layer 5/6 were compared between the control and post-sound situations. In total, 239 cells were recorded during different experiments out of which 124 neurons belonged to the layer 2/3 and remaining 115 to the layer 5/6. These pools were used for further analysis and statistics.



## Results

### Impact of repetitive auditory input on orientation tuning of visual neurons: A typical example

Unlike previous studies where a modulation of response was remarked after the presentation of auditory stimulus for a few milliseconds (Iurilli *et al.*, 2012; Ibrahim *et al.*, 2016), intriguingly, in this investigation, a complete shift in the Gaussian curves of the orientation tuning of neurons was observed following the sound application. Figure 3 shows the typical result of a recorded neuron pair from layer 2/3 and layer 5/6. Two typical orientation tuning curves in raw forms are shown as (A) and (C) for layer 2/3 and layer 5/6 respectively. To infer the exact value of orientation preference, non-linear Gaussian fits were generated and are shown for the supragranular (Figure 3B) and infragranular cell (Figure 3D) for either condition. It must be emphasized that both cells were recorded simultaneously from the same electrode and the recording sites were separated by ~500 microns. The supragranular cell exhibited an optimal orientation at 94.29° deg while the optimal orientation of the infragranular layer was 96.70° suggesting that the electrode was lowered in the same orientation column. Following sound application, both cells displayed a novel optimal orientation. The peak of the optimal orientation of the supragranular cell shifted to 110.92° indicating a displacement of 16° whereas the peak of the infragranular cell moved in the opposite direction to 74.94° demonstrating a shift amplitude of 21°. The opposite displacement of the peaks of optimal orientation tuning suggests that these shifts cannot be attributed to a global and spontaneous fluctuation of the firing rates. Each cell behaved independently. Furthermore, numerous studies have shown that, while the magnitude of the optimal responses may vary, the optimal orientation preference exhibits stability. Indeed, the optimal orientation remains same for hours and even days and these controls were shown from our lab by Bachatene and colleagues (Bachatene *et al.*, 2015). Similar results have been demonstrated by (Henry *et al.*, 1973; Frenkel *et al.*, 2006; Lutcke *et al.*, 2013). Therefore, the significant change in selectivity is due to the experience of visual neurons with the sound.

### Shift amplitude and sound source localisation

The extent of shift amplitude of the orientation tuning curves is illustrated in Figure 4. The shift amplitudes were calculated by subtracting the numerical values of orientation selectivity obtained at control and post-sound conditions. Color codes are respected throughout the figure. Pink and green are attributed to layer 2/3 and layer 5/6 respectively. On this data set, a non-parametric statistical approach was applied. The significant differences are indicated by solid black lines above each plot. The graphs A-D have measured values of orientation tuning when speakers were placed laterally on either side of the animal with respect to the fixation axis of the animal. A graph showing the orientation tuning values for all layer 2/3 neurons at control and post-sound presentation conditions are displayed. Significant differences deduced from Wilcoxon matched-pairs signed rank test (P value <0.0001) indicate the

difference between the two conditions is mostly significant. In supragranular, all cells (but one) (refer Figure 4 A) preferred orientations appear to have an incline towards horizontal axis (range  $0^\circ$  to  $50^\circ$ ). This bias may be contrasted with changes of preferred orientations in infragranular layers where the spread of covers the full extent (range  $0^\circ$  to  $157.5^\circ$ ). The significant bias observed could be attributed to the properties of the stimulus itself or to the distinct mechanism that drives the multimodal interaction between auditory and visual cortex. Next, shift magnitudes of neurons in either layer were compared (Figure 4 C). The mean shift amplitude for layer 2/3 and layer 5/6 neurons was found to be  $50.54 \pm 3.05$  (mean  $\pm$  SEM) and  $37.72 \pm 2.66$  respectively. Mann-Whitney test was applied to measure significance between the two populations, and the P value was found to be 0.0019. This comparison further demonstrates that layer 2/3 neurons exhibit more plasticity by changing their orientation preferences towards a variety of stimuli. Further, mean shifts of all four groups being layer 2/3 control and post sound and layer 5/6 control and post-sound were compared using One-way ANOVA (Figure 4 D). The means (mean  $\pm$  SEM) for the mentioned four data sets were  $81.41 \pm 4.95$ ,  $18.15 \pm 1.88$ ,  $83.33 \pm 4.56$  and  $71.38 \pm 4.33$  respectively. Tukey's multiple post comparison tests revealed three compared groups namely layer 2/3 control versus layer 2/3 post-sound, layer 2/3 post-sound versus layer 5/6 control and layer 2/3 post-sound versus layer 5/6 post-sound were significantly different whereas the remaining three groups namely layer 2/3 control versus layer 5/6 control, layer 2/3 control vs layer 5/6 post-sound and layer 5/6 control versus layer 5/6 post-sound were found statistically non-significant.

To explore the effects of displacement of the sound source, the speaker was positioned in the front of the animal. No critical differences in results were noticed in the orientation tuning values at both conditions for layer 2/3 neurons (N = 08, Figure 5A) and layer 5/6 neuron's (N = 11, Figure 5B). Here our aim was not to compare cells to cells obtained for two locations but to explore the differences in the pattern of response towards new location of the speaker. The significance was calculated using Wilcoxon matched-pairs signed rank test (P-value = 0.8984). Comparison of the mean of amplitudes at control and post-sound conditions for the four groups being layer 2/3 control and post sound and layer 5/6 control and post-sound were done using One-way ANOVA (Figure 5C), and no difference was found between results obtained with either location. The means (mean  $\pm$  SEM) for the mentioned four data sets were  $69.34 \pm 13.21$ ,  $14.79 \pm 4.90$ ,  $90.22 \pm 11.91$  and  $91.24 \pm 11.38$  respectively (Figure 5 D). A post comparison test disclosed three groups namely layer 2/3 control vs layer 2/3 post-sound, layer 2/3 post-sound vs layer 5/6 control and layer 2/3 post-sound vs layer 5/6 post-sound significantly different whereas the remaining three groups namely layer 2/3 control vs layer 5/6 control, layer 2/3 control vs layer 5/6 post-sound and layer 5/6 control vs layer 5/6 post-sound were found statistically non-significant at the same confidence level. These results were also comparable to results obtained when the speaker was placed on the sides of the animal.

Together, these results showcased the extended plastic nature of layer 2/3 neurons over layer 5/6 neurons and confirmed the independence of response change when the position of sound source was modified.

### **Sensitivity of Gaussian tuning curves towards sound: Layers behave alike**

The sharpness of orientation selectivity can be evaluated by measuring the bandwidth at half height of the orientation Gaussian tuning curve (Ringach *et al.*, 2002; Moore *et al.*, 2005). Here, we compared the tuning bandwidth of all neurons in either layer in control and post-sound conditions. Figure 6 is a compilation of bandwidth analyses on layer 2/3 and layer 5/6 neurons. Figure 6 A shows results for layer 2/3 neurons (N = 60). Overall, the tuning bandwidth at half magnitude (FWHM: full width at half magnitude) is slightly enlarged, but this increase in bandwidth was not found significant between the two conditions (Wilcoxon matched-pairs signed rank test, P-value = 0.0663). The increase of bandwidth of a neuron indicates broadening of selectivity for range of orientations signifying a large contribution of flank orientations in the overall tuning of the neuron. This result specifies that presentation of a repetitive sound impose neurons to gain a novel preference of orientation for more than one orientation at the same time. Such an increase in bandwidth strongly proposes that sound repetition induces the development of a different preferred orientation with a broader tuning curve. This effect can be further understood by relating the results observed in Figure 4 A where values of orientation preference for layer 2/3 cells held a bias towards the horizontal orientations after the sound protocol was applied. It appears as if the group of neurons recorded from each site was controlled by a mechanism that triggered on the application of sound for 12 min and thus all neurons in the superficial layer responded towards sound in the same way. Similarly, in Figure 6 B, layer 5/6 cells (N = 80) also showed a similar increment in the bandwidth responses, and the difference between the two groups was found highly significant (Wilcoxon matched-pairs signed rank test, P-value = 0.0697). Neurons in a cortical column generally exhibit similar conduct towards stimuli features but it is also familiar that response towards stimulus properties decrease with increasing depth down the column. Therefore, a mechanism parallel to both layers could be held responsible for the change in bandwidth but feeble selectivity in deeper layer. Further, Figure 6 C reveals the subtractions in bandwidth at two given circumstances (control and post-sound) for both layers. The means for layer 2/3 and layer 5/6 were  $24.07 \pm 3.58$  and  $56.13 \pm 4.60$  respectively and were tested to be significantly different (P value < 0.001) as an outcome of Mann-Whitney test. This suggests that though both layers displayed similar behavior towards the sound stimulus nonetheless layer 5/6 cells deviated more in comparison to layer 2/3. Finally, the mean values of neurons' bandwidths were compared to each other in both layers. This is displayed in Figure 6 D. All four groups being layer 2/3 control and post-sound and layer 5/6 control and post-sound were scrutinized using One-way ANOVA. The means (mean  $\pm$  SEM) for the mentioned four data sets were  $17.53 \pm 2.29$ ,  $28.14 \pm 3.59$ ,  $22.74 \pm 2.73$  and  $72.52 \pm 4.38$

respectively. Tukey's multiple post comparison tests revealed that out of total, two groups namely layer 2/3 post-sound vs layer 5/6 post-sound and layer 5/6 control vs layer 5/6 post-sound had P-value <0.05, thus means were fairly high for layer 5/6 whereas for groups layer 2/3 control vs layer 2/3 post-sound and layer 2/3 control vs layer 5/6 control means were found statistically non-significant at the same confidence level. In summary, these results showed a global deviation of layer 5/6 cells with higher means of bandwidths.

### **Orientation Selectivity Index (OSI)**

In line with the previous reports ([Dragoi et al., 2001](#); [Ringach et al., 2002](#); [Atallah et al., 2012](#); [Denman & Contreras, 2014](#)) neurons having an OSI superior or equal to 0.4 can be classified as sharply tuned cells. However, in this investigation OSI values for all cells have been pooled to generate the figure. Figure 7 is a pool of layer 2/3 and layer 5/6 neurons. Figure 7 A shows results for layer 2/3 neurons. Each layer 2/3 neuron (N = 124) is displayed in the figure. Overall, the OSI remained same which indicates that the new selectivity acquired by the neuron was as robust as the initially preferred. Layer 5/6 neurons displayed a similar pattern of the result. However, if layer 2/3 neurons are compared to layer 5/6 neurons, the deviation for layer 2/3 neurons (Wilcoxon matched-pairs signed rank test, P-value = 0.0663) was found more. Thus, layer 5/6 experience more dispersed evoked response towards all presented orientations (Figure 7 B). Figure 7 C concludes the tendency between superficial and deeper layers. Layer 2/3 and layer 5/6 neurons altered with a minute mean of OSI which suggests that layer 5/6 neurons experienced more change in OSI. The comparison between means also conveyed the same outcome of layer 5/6 experiencing a decline in selectivity to preferred orientation (Figure 7 D). These results also correspond to our bandwidth data. The broadening of tuning curves after the imposition of sound lead to decrease in mean OSI.

### **Response change index (RCI) : Response modulation comparison between orientations**

As described in methods section the modulation of response magnitude was calculated for all cells and for all applied oriented gratings. Results are compiled in Figure 7. The mean RCI (mean  $\pm$  SEM) of all layer 2/3 and layer 5/6 neurons (Figure 8 A) were uncovered to be  $-0.03435 \pm 0.02$  and  $0.03098 \pm 0.02$  and found statistically non-significant (Mann Whitney Test, P-value = 0.0682). Altogether, layer 2/3 experienced response suppression and layer 5/6 experienced response enhancement. This analysis, however, unveils more exciting results. Indeed, in supragranular layers, the firing rate decreases for most orientations whereas in infragranular an opposite effect is observed. However, the variation is unbalanced when one computes RCI orientation by orientation. However, in layer 2/3 responses fluctuate roughly with the same magnitude for all tested orientations The differences between all possible pairs among all

orientations were measured by one-way ANOVA and a post ANOVA test (Tukey's multiple comparison tests was applied to compare variances among means (Figure 8 B). The differences between all orientations in layer 2/3 were found non-significant. Remarkably in layer 5/6 the largest RCI was calculated for orientations close to the vertical axis (Figure 8 C). As the latter departs from vertical alignment, the RCI regularly declines to become negligible when grating reaches the horizontal axis. Few compared groups tested significantly. For rest of the groups, the mean of RCI was not significantly different. This striking inverse response modifications of layer 2/3 and layer 5/6 neurons may be attributed to changes of excitation and inhibition during the presentation of sound. Furthermore, this inverse result also highlights the anticipated independent nature of superficial and deeper layers in the cortical column.

## Discussion

The present study aimed to investigate the responses of visual neurons of V1 when stimulated by a repetitive auditory stimulus whose frequency and power varied cyclically and which presumably drove many putative synaptic inputs. The investigation revealed that continuous cyclical sound application in isolation brings out three main results. First, we observed shifts in the peaks of orientation tuning curves in cat's supra -and infragranular layers implying a novel orientation selectivity. Second, superficial and deeper layers seemed to behave independently although both were recorded in the same columns at the same time. Moreover, cells in both layers were sometimes found shifting in an opposite direction. Third, neurons in infragranular layer 5/6 exhibit larger shifts. This suggests that neurons in the primary visual cortex (V1) are not merely extractors of visual features but respond well to non-visual information (Shuler & Bear, 2006; Keller *et al.*, 2012; Poort *et al.*, 2015).

## Supramodal nature and cross-modal plasticity in the cortex

Our results augment cross modalities and further amplify the observations made by previous investigations in this direction. Unlike the slight modulation of response in terms of firing rate of neurons detected in previous investigations (Jurilli *et al.*, 2012; Ibrahim *et al.*, 2016), we observed a much more intense response in our data wherein V1 neurons experienced a complete change in their orientation preference. This kind of modification is earlier reported in literature related to adaptation studies where neurons imposed with an adapting orientation undergo a learning process and finally acquire the imposed adapter as the new preferred selectivity. These visual adaptation protocols pertain to the classical flow of information involving LGN, projecting the input to layer 4 of the primary visual cortex and further delivering the information to layer 2/3 and finally layer 5/6. Fascinatingly, in the current case, similar results were obtained. Indeed, in this case, it is the application of sound for several minutes that induced neurons to acquire a different preferred orientation even when exposed to a non-visual input. Interestingly,

the present study involves a non-geniculate direct pathway. Comparing the two effects, it is indeed intriguing how cortex displays various possible avenues to acquire the outside information. The initial set of questions that enthralls the brain are; is this because the perceived sound stimulus by the animal generates a visual format of the sound stimulus thus eliciting an intense response in the visual neurons? Is it because visual cortex can inherently respond to an auditory stimulus since it is inherently supramodal in nature? Is it that cortex responds to the context of presented sound stimuli? Alternatively, is it a combination of all these possibilities? Though the principle underlying such interactions have not been fully discovered yet the most suitable explanation that fits in with the results is the combination of cross-modal plastic mechanisms and supramodal nature of the visual cortex. It is known for decades that visual cortex is a stimulus-driven structure due to which visual cortex exhibits unique response patterns towards different protocols and stimuli. It should be stressed enough that visual cortex was able to respond distinctively to environments because it inherently could do so. Perhaps this ability was induced during developmental stages and developed with experience. It seems likely that cross-modal interactions are recruited more often in early blinds or congenital blinds where there is an urgent need for another sensory modality to take over the responsibility to trigger processing at early stages and then also employ the visual cortex to respond in full capacity. In this case, a reorganization of the cortex is generally noted for a recalibration of the sensory system. In the present study, healthy animals were monocularly stimulated. Therefore the possibility of undergoing a supramodal mechanism supported by a cross-modal communication between sensory structures seems more reasonable. It is hypothesized that, upon sensory activation, the visual cortex relies on the abstract representation of the sensory stimuli regardless of the sensory modality. It might also happen that upon triggering by a sound stimulus, which is our case, both visual and auditory cortices are engaged cross-modally and both approaches exist together. A related line of thought by Muckli and colleagues (Muckli *et al.*, 2015) further highlights that a significant source of information lies in the context of the stimuli. Any sensory stimuli involving a feature can potentially embody the global features of the stimuli that are enough to trigger a complex scene representation of the same sound stimulus in the visual cortex (Bar, 2004; Oliva & Torralba, 2007), especially when presented for a prolonged duration. Therefore, feedback triggered by the sound stimulus may use coarse information from the stimulus property involving the visual cortex in the processing. Raw signals may carry information about the overall structure of the scene in the form of contours, and this rough representation can help to segment the scene and boost the recognition process within the scene associated with that specific sound. It is thought-provoking, considering the intense interconnectivity within and between different sensory areas of the cortex. Although these effects have been discussed mainly from imaging studies on humans, the underlying principle can undoubtedly be applied to our data (Vogels, 1999; Muckli *et al.*, 2005; Vetter *et al.*, 2014; Muckli *et al.*, 2015).

### **Inhibitory mechanisms**

Recent studies have suggested that sound modulates light responses by impacting inhibitory neurons in V1 (Iurilli *et al.*, 2012; Kayser & Remedios, 2012; Pluta *et al.*, 2015; Ibrahim *et al.*, 2016). A very recent report (Deneux *et al.*, 2018) has revealed that auditory cortex neurons project to V1 inhibitory neurons in the superficial layers especially layer 1. These interneurons act as initiating points and passage for a cross-modal stream that recruits a suppressive approach of processing. This specific pathway is activated precisely in response to only non-visual inputs (Deneux *et al.*, 2018). Further, they found that specific interneurons that generate inhibition simultaneously conceal the excitatory drive from auditory cortex to V1 (Deneux *et al.*, 2018). They reported that the inhibitory mechanism observed originated in a dark setup yet the results could be applied in the current investigation since the experiments were also performed similar conditions. The most important result from their study unveiled that only the inhibitory neurons in superficial layer 1 of the primary visual cortex consist of a subpopulation of GABAergic neurons that are implicated in sound-induced inhibition. Further, they added that these interneurons process context-dependent information and produce inhibitions upon meeting the action potentials from A1 (Deneux *et al.*, 2018). Infragranular layers might not be comprised of these specialized interneurons. Further, it has been (Iurilli *et al.*, 2012; Ibrahim *et al.*, 2016) shown that sound excites GABAergic cells in V1 which in turn hyperpolarize pyramidal neurons and suppress evoked light responses. Hyperpolarizing pyramidal cells may lessen their excitation upon interaction with inhibitory cells and in turn, further weakens cross-orientation inhibition via a disinhibition process. Such steps allow change of preferred orientation into another optimal orientation that may lead to shifts of selectivity. Therefore, this could explain how neurons maintain inhibition in visual cortex for the entire stimulation process of 12 minutes. Henceforth, in most cases, audio-visual interactions are disclosed by modulations of the magnitude of evoked responses to visual targets in the presence of sound. On similar lines, it has been hypothesized that sound exerts a divisive or additive influence, resulting in a decline or enhancement of light responses (Pluta *et al.*, 2015). In general, the suppressive effects are more frequently reported in response to light. Moreover, it has been observed that simultaneous presentation of acoustic and visual stimuli to the test neurons triggers a competition between the two sensory inputs; auditory and visual (Kayser & Remedios, 2012; Yates, 2012).

### **Layer 2/3 and layer 5/6 neurons change orientation preferences**

In line with the previous studies in visual adaptation, many authors have described shifts of optimal orientation tuning or changes in orientation selectivity after a short (less than a minute) (Dragoi *et al.*, 2000) or long light adaptation (Ghisovan *et al.*, 2008; 2009; Bachatene *et al.*, 2012b; Bachatene *et al.*,

2013; Bachatene *et al.*, 2015; Chanauria *et al.*, 2016) (several minutes). Usually, the protocol requires the frequent or continued application of a non-preferred property of the adapter such as orientation. In the above experiments, the peak of the orientation tuning curve is displaced either toward (attractive) or away (repulsive) from the adapting orientation. In all cases, such protocol results in the emergence of a novel orientation selectivity. It has also been demonstrated before in one of our previous studies (Chanauria *et al.*, 2016) that layer 2/3 and layer 5/6 neurons work in parallel towards the adapter orientation and thus neurons in either layers can attain new selectivity following adaptation. Neurons undergo push-pull mechanism (Bachatene *et al.*, 2012b; Bachatene *et al.*, 2013; Bachatene *et al.*, 2015; Chanauria *et al.*, 2016) that is based on the decrease and increase of the firing rates towards initially preferred and adapting orientation respectively.

In the current investigation, the non-preferred stimulus traditionally referred to as visual adapter, is absent and is replaced by exposure to a sound stimulus imposed in seclusion for several minutes uninterruptedly wherein responses of individual visual neurons are recorded before and after the sound application and compared. Results revealed that such presentation of sound not only modulates visual responses but entirely shifts the orientation tuning curves of individual visual neurons in supra and infragranular layers of area 17 of cats. Consequently, the sound seemed to exert distinctive effects in addition to global modulatory influence. As orientation selectivity is shaped at the cortical level, thanks to aligned thalamic inputs upon cortical recipient neurons, the changes of orientation selectivity are unlikely to happen at thalamic levels where cells have mostly concentric receptive field (although some units may exhibit a slight orientation bias). Further, we found populations of neurons (layer 2/3 and layer 5/6) exhibiting enhanced or diminished responses while the overall response of the population remained balanced (Figure 7A). Especially, at 90° orientation, a clear enhancement of response is noticed wherein layer 2/3 neurons exhibited suppression and layer 5/6 experienced increase of excitation.

It has been noted that when sound presented solely, produces weak visual responses (Deneux *et al.*, 2018; Daniel, 2011). A threshold mechanism responsible for eliciting stronger responses in V1 could be achieved if enough visual input reach V1 and overpass required strength of interaction. This kind of mechanism can logically happen in layer 2/3 where pyramidal neurons receive direct inputs from auditory cortex as 12 min time is enough to encode the raw embedded visual information within the audio stimulus. The underlying principle explained above can undoubtedly be applied in the current scenario. The bias we observed could be a consequence of such a process, and that is why we do see an evident response bias towards horizontal for layer 2/3 neurons but not in layer 5/6. The bias could also be inherently induced because of the property of the sound itself. Therefore, to understand the bias towards horizontal orientations a complete set of experiments need to be performed with different types of sounds which will be another enormous set of experimentation. Another important revelation from a previous study (Deneux



*et al.*, 2018) was that as the intensity of sound increases the response gets stronger. The intensity of the stimulus we used was kept same for the 3s, and the same 3s were repeated throughout 12 min, therefore, with every repetition the representation of the information embedded in sound became dominant thus we saw an intense change of selectivity and not just a modulation of firing rate. However, the responses of cells activated in response to the sound respond non-linear towards the duration of the sound presented (*Xu et al.*, 2012).

Ibrahim and co-authors (*Ibrahim et al.*, 2016) demonstrated that layer 2/3 neurons get suppressed by the A1 signals which are what was found in our data too. Layer 2/3 neurons keep receiving the information for 12 min and presumably the intensity of the inhibitory drive increase with duration of stimulation. In this scenario, another feedback drive initiates in A1 and interacts with layer 5/6 neurons that further maintain the influence on layer 2/3 cells. (*Fritz et al.*, 2003; *Muckli & Petro*, 2013; *Vetter et al.*, 2014; *Muckli et al.*, 2015; *Ibrahim et al.*, 2016). Therefore, it appears that layer 2/3 suffers extreme inhibition whereas layer 5/6 neurons experience more excitation.

### **Layers behave as separate compartments**

Our results disclosed another important original result. The sound seemed to contribute to the layout of orientation maps in V1. It has been demonstrated that fibers emerging from auditory cortices activate mostly GABAergic inhibitory cells which in turn hyperpolarize pyramidal cells in both infra and supragranular layers in visual cortex (*Ibrahim et al.*, 2016). There are direct and indirect connections arising from V1 and ending at different areas in the cortex, almost covering the entire cortex and making it reciprocally interconnected (*Petro et al.*, 2013; *Petro et al.*, 2017). As electrodes were introduced orthogonally in area 17 and thus presumably each recording site in either layer (layers 2/3 and 5/6) was in the same orientation column, the dual projection in supra and infragranular layers may elucidate shifts of the peak of tuning curves in the opposite direction (see example tuning curve). Another important observation that was discovered in our data was the bias for layer 2/3 neurons for horizontal orientations after the experience with sound. This intriguing effect may be attributed to firstly the property of sound itself. It has been known for many years now that visual cortex is a stimulus-driven structure (*Doron et al.*, 2002; *Izraeli et al.*, 2002; *Piche et al.*, 2007; *Chabot et al.*, 2008). The non-visual information in the stimulus can transmit from non-visual sensory structures to visual cortex by direct corticoccipital pathways and circumvent the higher order cortex. Further, in this situation, the nonvisual signals do not undergo a modulation but only translate the stimulus-driven information. Xu and co-authors (*Xu et al.*, 2012) suggested that functional mixing of inputs from two different sources could allow for facilitative non-linear interactions within individual dendrites that may lead to the bias towards horizontal orientations. This non-linearity may clarify a preference towards the horizontal orientations.

## **Conclusion**

Undeterred by the traditional view of sensory processing that restricts the merging of sensory information only to higher association cortices, latest reports suggest that the early visual cortex is also involved in the integration of multimodal information. Nevertheless, a crucial and detailed inspection is required to fully fathom the mechanisms of cross-modal integration in primary sensory areas especially the primary visual cortex. Together, our data demonstrated that visual cortical neurons can respond to sound stimulations in the absence of any visual inputs in a strong manner that leads single neurons to undergo an alteration of selectivity. Further, understanding cross-modal plasticity employs specific pathways within and between sensory areas to process diverse inputs and response towards outside environment can be varied. A model of possible mechanisms underlying our observations have been displayed as Figure 9. The model has been adapted from papers already cited in the text.

## **Figure and legends**

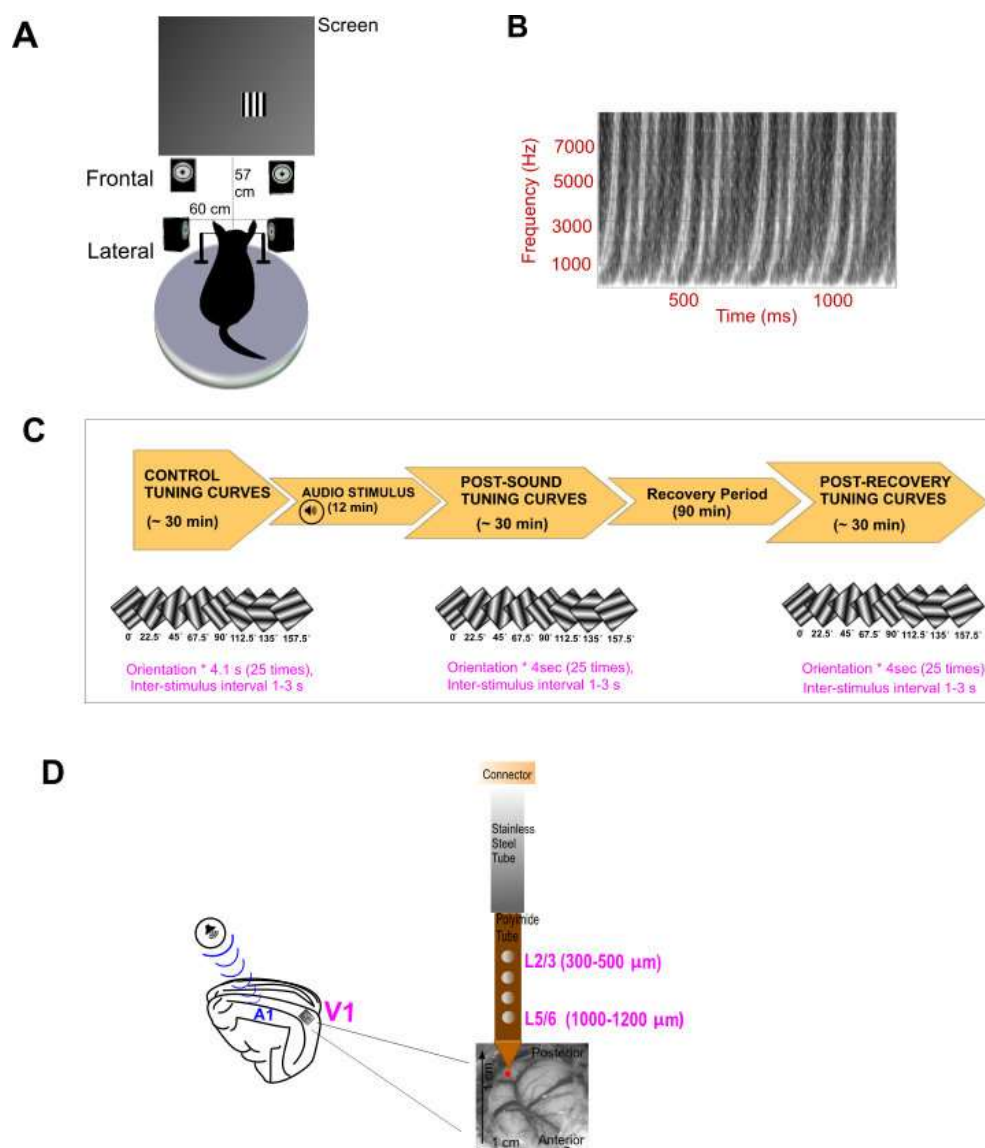


**Figure 1**

Experimental set up of stimulation, neuronal recordings and sound stimulus (A) Cartoon of the anesthetized cat fixed on the stereotaxic apparatus. Visual stimulus (shown as black and white gratings) is presented inside the receptive fields of test neurons. The sound stimulus is delivered by a pair of speakers placed frontally and laterally to the axis of the animal (B) The spectrogram of the sound stimulus is displayed. The spectrogram shows that frequencies are played with a constant frequency modulation (FM) pattern. (C) A pictorial representation of the steps followed during the protocol. Two types of stimuli were applied: Visual and auditory. Visual stimuli (sine-wave drifting orientation-gratings) were presented in a random order. Each stimulus was presented 25 times and each trial lasted 4 s with a 1–3-ms inter-stimulus interval followed by delivery of sound stimulus for 12 min. The same set of visual stimuli is shown again in a random order. A recovery period of 90 min is offered after which the gratings are presented again (D)

Illustration of the electrode used in the experiments. Neurons are recorded using multichannel depth electrode from 300-500  $\mu\text{m}$ , and 1000-1200  $\mu\text{m}$  from the primary visual cortex (V1) or area 17 before and after auditory cortex is stimulated by the presentation of sound

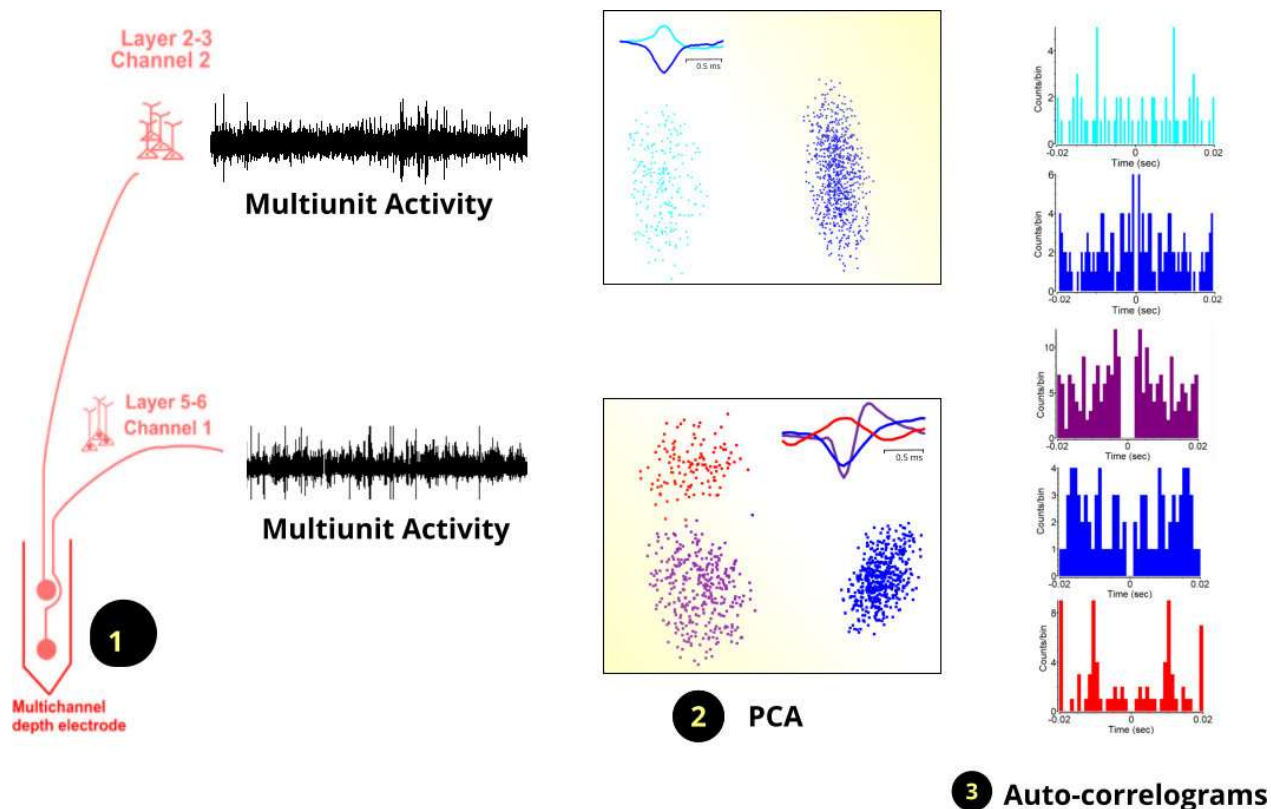
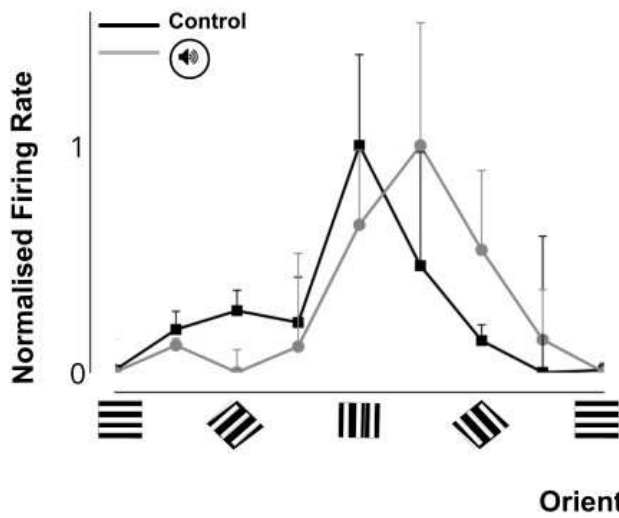


**Figure 2**

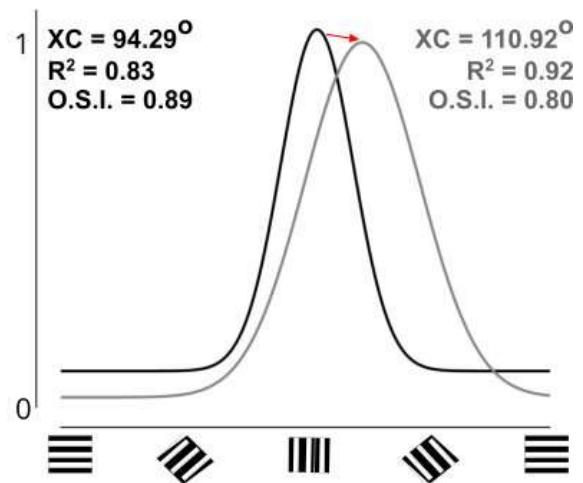
An example of the spike sorting process for isolation of single units is exhibited. Part 1 displays that the neurons have been recorded simultaneously from layer 2/3 and layer 5/6 of the V1. Multiunit activity from either layer is also displayed alongside. Part 2 shows the cluster analysis of the dissociated waveforms. Part 3 displays the auto-correlograms for the separated single units. No events at zero represent the refractory period of neuron that confirms the individuality of each neuron. Further, superimposed average waveforms of dissociated spikes from multi-unit recordings have been shown against the black background.

## LAYER 2/3

### A Raw Tuning Curves

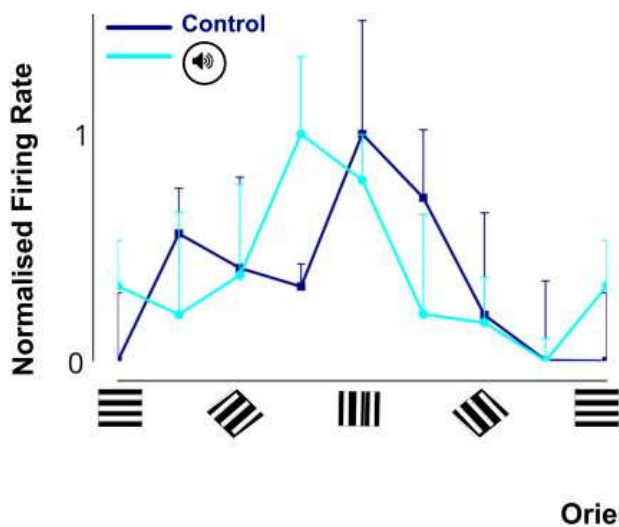


### B Gaussian-fits



## LAYER 5/6

### C Raw Tuning Curves



### D Gaussian-fits

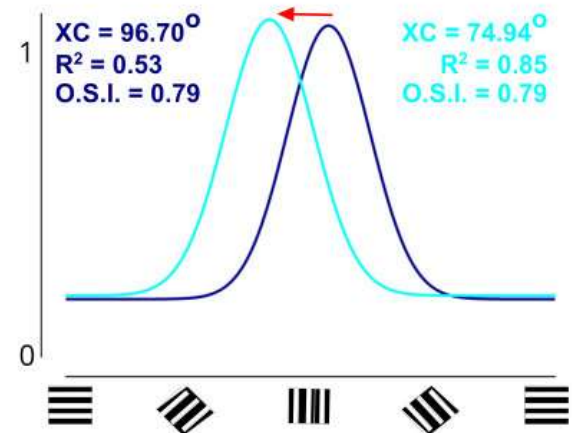


**Figure 3**

Typical examples of shifts of orientation tuning curve peaks. The figure represents a pair of layer 2/3 and layer 5/6 neurons recorded simultaneously during the task. Color codes are displayed alongside the curves. The bars signify standard error of the mean (mean  $\pm$  SEM) over 25 trials at each presented oriented grating. The direction of shift is highlighted by small red arrow (A) Raw orientation tuning values are compared for layer 2/3 neuron at control and post-sound conditions in black and grey respectively. A clear

change in selectivity can be observed (B) To deduce the exact values of orientation tuning raw values were fitted using the Gauss function. An overlap of the initially preferred and the new selectivity has been depicted by using XC and  $R^2$ . OSI values are also mentioned (C) Raw tuning curves of layer 5/6 neuron at control and post-sound conditions are displayed in navy and cyan colors respectively (D) Gaussian fitted tuning curves for layer 5/6 neuron over raw data is shown.

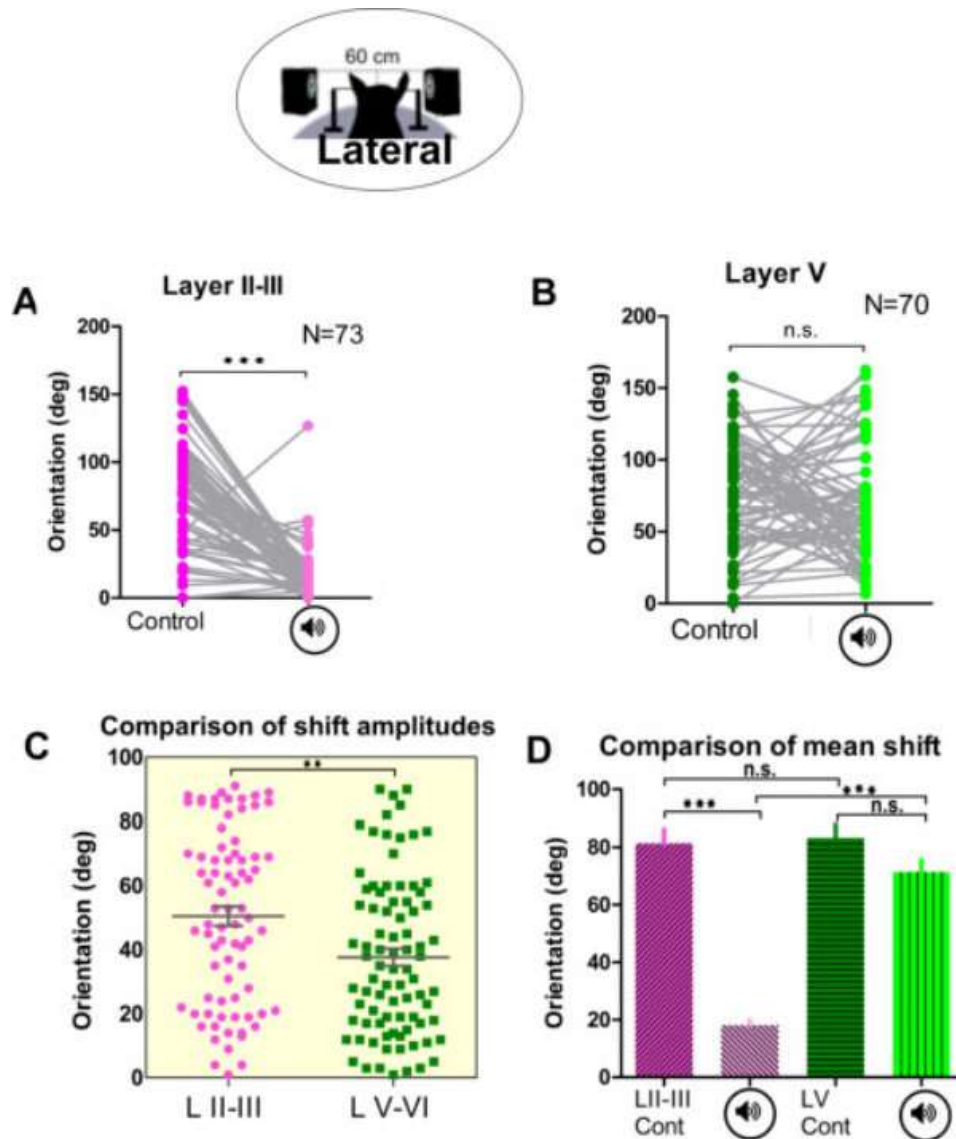


**Figure 4**

Acoustic stimulation results in deviation of orientation preference and modulation of shift-magnitudes in V1 orientation columns. Here we show shift magnitudes for all analyzed neurons in either layer. Pink and green colors indicate layer 2/3 and layer 5/6 respectively. This population data did not pass the Shapiro-Wilk normality test and consequently non-parametric statistical approach was followed. The significant differences are indicated by solid black line above each plot. The graphs A-D are measured values when speakers were placed on the either side of the animal with respect to the fixation axis of the animal (A) A plot of orientation tuning values for all layer 2/3 neurons (N=73), as individual units, at control and post-sound presentation conditions is displayed. Significant differences deduced from Wilcoxon matched-pairs signed rank test (P value <0.0001) (B) A similar plot of orientation tuning values for all layer 5/6 neurons



(N=70), as individual units, at control and post-sound presentation conditions is shown. The significance was calculated using Wilcoxon matched-pairs signed rank test (P-value = 0.02280) (C) A graph showing shift magnitudes in either layer as a result of imposition of sound. The mean shift amplitude for layer 2/3 and layer 5/6 neurons were found to be  $50.54 \pm 3.051$  (mean  $\pm$  SEM) and  $37.72 \pm 2.661$  respectively. Mann-Whitney test was applied to measure significance between the two populations and the P value was found to be 0.0019. (D) Graph showing mean of amplitudes at control and post-sound condition. All four groups layer 2/3 control, layer 2/3 post-sound, layer 5/6 control and layer 5/6 post-sound were compared in this analysis using One-way ANOVA. The means (mean  $\pm$  SEM) for the mentioned four data sets were  $81.41 \pm 4.952$ ,  $18.15 \pm 1.882$ ,  $83.33 \pm 4.566$  and  $71.38 \pm 4.332$  respectively. Further, with the help of Tukey's multiple post comparison test, the differences between one data set with the other three at a time was calculated. Three compared groups namely layer 2/3 control vs layer 2/3 post-sound, layer 2/3 post-sound vs layer 5/6 control and layer 2/3 post-sound vs layer 5/6 post-sound had P-value  $<0.05$  whereas the remaining three groups namely layer 2/3 control vs layer 5/6 control, layer 2/3 control vs layer 5/6 post-sound and layer 5/6 control vs layer 5/6 post-sound were found statistically non-significant the same confidence level.

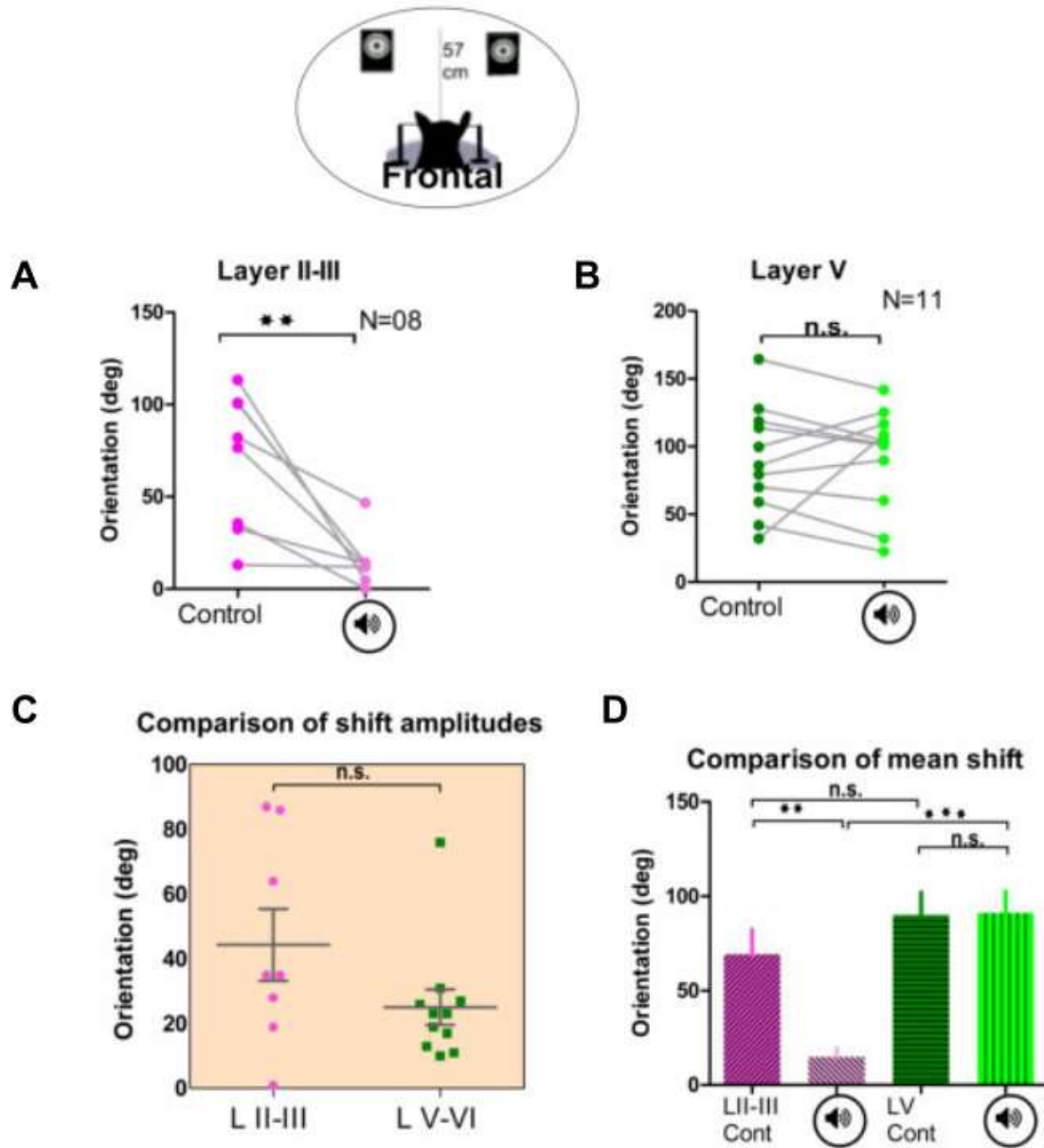


**Figure 5**

Graphs A to D show results when the speaker were positioned in the front of the animal. A non-parametric statistical approach was followed since the data did not pass the normality test (A) Orientation tuning values are plotted at both conditions are plotted for each layer 2/3 neurons (N = 8), statistical differences deduced from Wilcoxon matched-pairs signed rank test (P-value = 0.0078) (B) Each layer 5/6 neuron's (N = 11) orientation tuning values are displayed in the graph. The significance was calculated using Wilcoxon matched-pairs signed rank test (P-value = 0.8984) (C) Graph showing shift magnitudes in either layer after of imposition of sound. The mean shift amplitude for layer 2/3 and layer 5/6 neurons were

found to be  $44.38 \pm 11.10$  (mean  $\pm$  SEM) and  $25.09 \pm 5.490$  respectively. Mann-Whitney test was applied to measure significance between the two populations and the P value was found to be 0.0825 (D) Histogram of mean of amplitudes at control and post-sound conditions. The four groups being layer 2/3 control and post sound and layer 5/6 control and post-sound were compared using One-way ANOVA. The means (mean  $\pm$  SEM) for the mentioned four data sets were  $69.34 \pm 13.21$ ,  $14.79 \pm 4.908$ ,  $90.22 \pm 11.91$  and  $91.24 \pm 11.38$  respectively. Further, using Tukey's multiple post comparison test the differences between all groups was calculated. Three compared groups namely layer 2/3 control vs layer 2/3 post-sound, layer 2/3 post-sound vs layer 5/6 control and layer 2/3 post-sound vs layer 5/6 post-sound had P value  $P < 0.05$  whereas the remaining three groups namely layer 2/3 control vs layer 5/6 control, layer 2/3 control vs layer 5/6 post-sound and layer 5/6 control vs layer 5/6 post-sound were found statistically non-significant the same confidence level.

## BANDWIDTHS

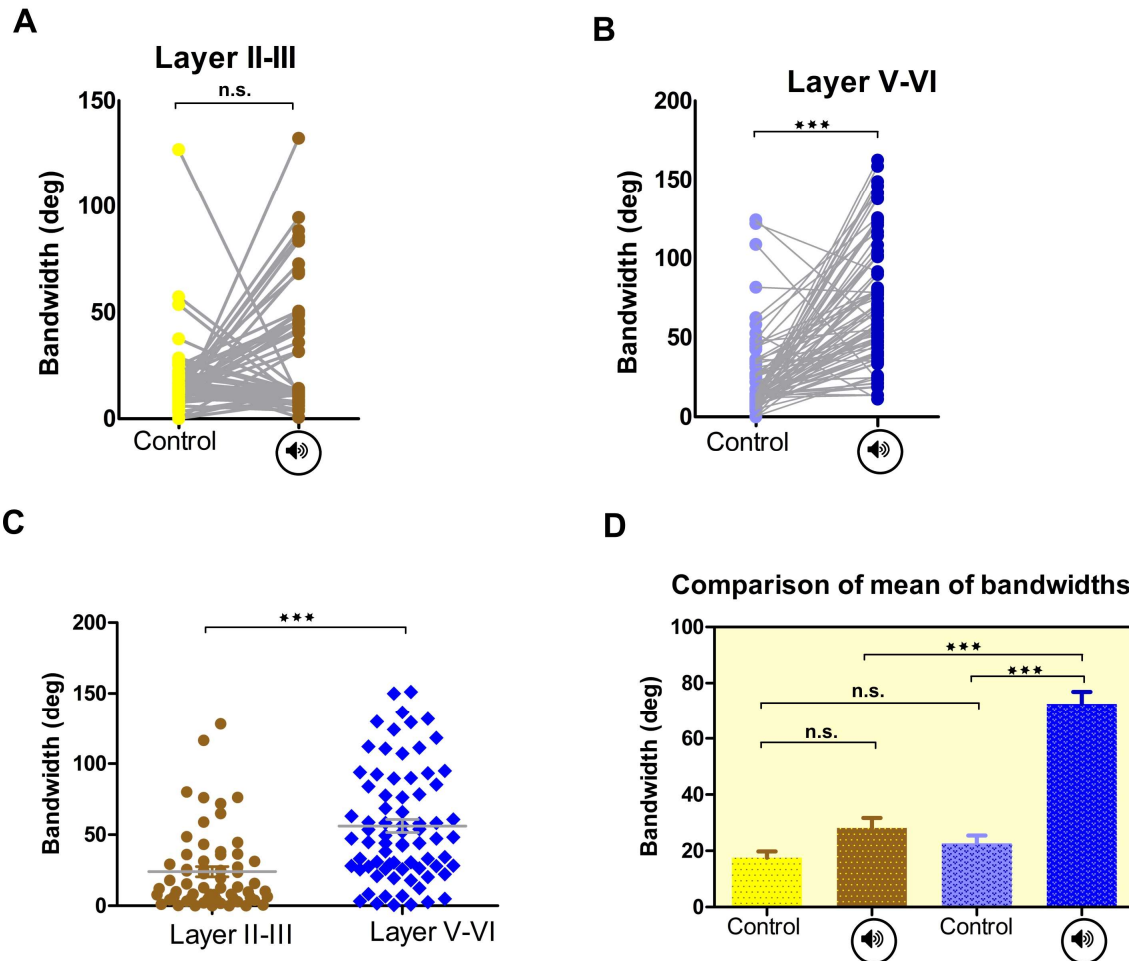


**Figure 6**

The sharpness of orientation selectivity. Brown and blue colors code for layer 2/3 and layer 5/6 neurons respectively. A non-parametric statistical approach was followed to measure significance between data sets (A) The numerical values of bandwidths plotted for each layer 2/3 cell (N = 60). Wilcoxon matched-pairs signed rank test (P-value = 0.0663) was applied (B) A similar plot of bandwidth values for all layer 5/6 neurons (N=80), as individual units, at control and post-sound presentation conditions is shown. The significance was calculated using Wilcoxon matched-pairs signed rank test (P-value = 0.0697) (C) A comparative graph showing differences of bandwidth between control and post-sound condition for either layer is arranged side by side. The means (mean  $\pm$  SEM) for layer 2/3 and layer 5/6 were measured as  $24.07 \pm 3.580$  and  $56.13 \pm 4.602$  respectively and were tested to be significantly different (P value < 0.001) as a result of Mann-Whitney test (D) Graph showing mean of bandwidths at control and post-sound

condition. All four groups being layer 2/3 control and post-sound and layer 5/6 control and post-sound were compared in this analysis using One-way ANOVA. The means (mean  $\pm$  SEM) for the mentioned four data sets were  $17.53 \pm 2.293$ ,  $28.14 \pm 3.595$ ,  $22.74 \pm 2.736$  and  $72.52 \pm 4.389$  respectively. Further, with the help of Tukey's multiple post comparison test the differences between all four data sets were calculated. Three groups namely layer 2/3 control vs layer 5/6 post-sound, layer 2/3 post-sound vs layer 5/6 post-sound and layer 5/6 control vs layer 5/6 post-sound had P-value  $<0.05$  whereas layer 2/3 control vs layer 2/3 post-sound, layer 2/3 control vs layer 5/6 control and layer 2/3 post-sound vs layer 5/6 control were found statistically non-significant the same confidence level.

## OSI

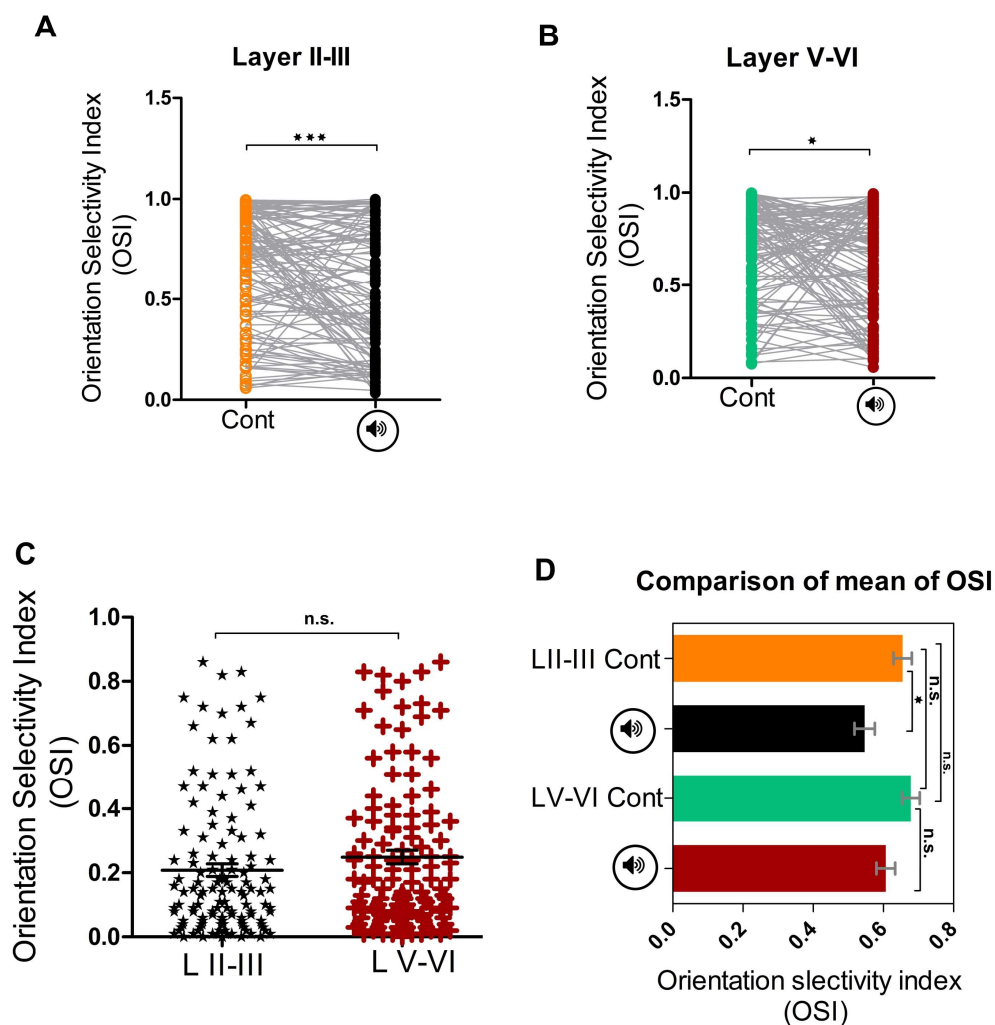


**Figure 7**

Orientation Selectivity Index (OSI). Yellow and black colors coded for layer 2/3 cells in control and post-sound situations whereas green and maroon colors indicate to the two respective conditions for layer 5/6 neurons. Further, in graph C the maroon and black colors code layer 2/3 and layer 5/6 neurons as shown in the figure. A non-parametric method has been adopted to measure differences between different populations (A) OSI values calculated for each layer 2/3 neuron (N = 124) at control and post-sound conditions have been displayed and were found significantly different (P value < 0.0001) after employing Wilcoxon matched-pairs signed rank test. (B) Similar symbol and line plot are also shown for all layer 5/6 neurons (N = 115) at both circumstances. Wilcoxon matched-pairs signed rank test revealed the P-value = 0.0216 (C) A similar strategy was followed to calculate differences between the OSI values of the two conditions for each layer. The means (mean  $\pm$  SEM) for both groups were found to be  $0.2081 \pm 0.01961$

and  $0.2491 \pm 0.02159$  and P value = 0.1106 from Wilcoxon matched-pairs signed rank test (D) Parallel to previous graphs the data values from either layer for both conditions is compared using One-way ANOVA. The groups having statistically different means at  $P < 0.05$  were control layer 5/6 vs post-sound layer 2/3 and post-sound layer 2/3 and control layer 2/3 whereas remaining groups were not found different at any significance level.

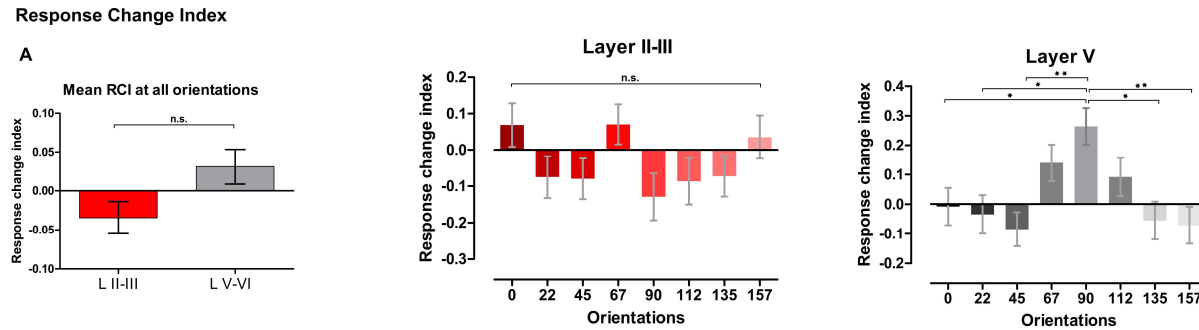


**Figure 8**

Response Change Index (RCI). Red and black colors indicate layer 2/3 and layer 5/6 respectively. A non-parametric method is opted for statistical validations (A) Histogram showing mean of RCI of all test neurons in either layer at all presented orientations ( $0^{\circ}$  -  $157.5^{\circ}$ , separated by  $22.5^{\circ}$ ). The mean RCI (mean  $\pm$  SEM) of all layer 2/3 and layer 5/6 neurons were found to be  $-0.03435 \pm 0.02054$  and  $0.03098 \pm 0.02241$  and statistically non-significant (Mann Whitney Test, P-value = 0.0682) (B) A graph showing histograms of RCI at different orientations for layer 2/3 cells. The differences between all possible pairs among all orientations were measured by one-way ANOVA and a post ANOVA test (Tukey's multiple comparison test) was applied to compare variances among means. (C) A similar, analysis was done on layer 5/6 neurons and histogram was generated. Few groups out of all possible paired comparisons tested significantly. They were  $0^{\circ}$  vs  $90^{\circ}$ ,  $22^{\circ}$  vs  $90^{\circ}$ ,  $45^{\circ}$  vs  $90^{\circ}$ ,  $90^{\circ}$  vs  $135^{\circ}$  and  $90^{\circ}$  vs  $157.5^{\circ}$ . For rest of the groups, the mean of RCI was not significantly different.



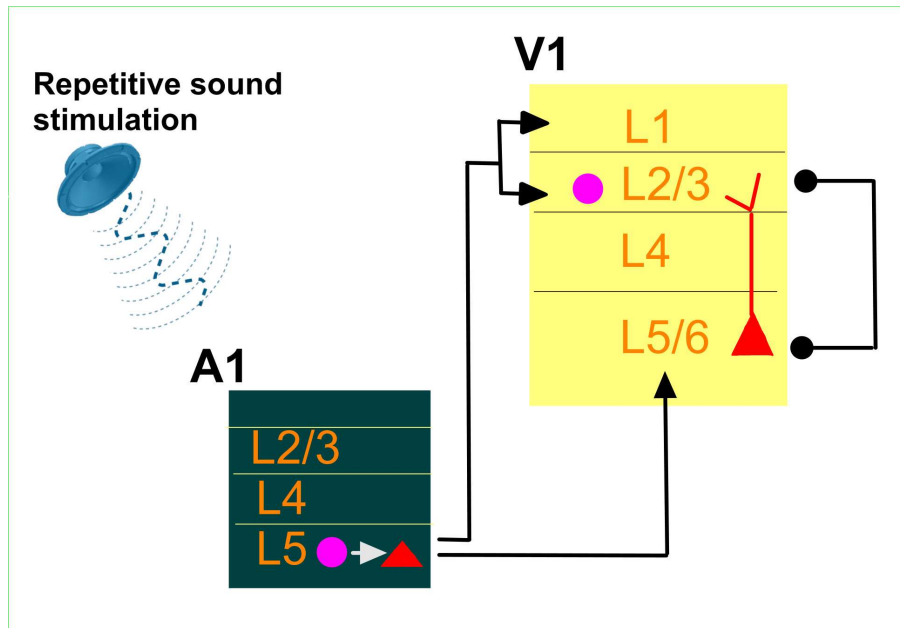


**Figure 9**

A model of possible neural mechanisms taking place during the sound only protocol applied that justify the deviation in the orientation tunings of individual neurons in supra and infragranular layers in the V1 cortical column. The illustration is adapted from different studies that were discussed throughout the paper. On the onset of sound, A1 gets activated and projects directly on superficial layers of the V1. A1 projections recruit GABAergic cells in layer 2/3 of V1 and generate inhibition within this interaction. During this process layer, 2/3 cells and layer 5/6 cells interact because of disinhibition where both layers inhibit each other. In another case, auditory cortex might directly project on layer 5/6.

## References

Atallah, B.V., Bruns, W., Carandini, M. & Scanziani, M. (2012) Parvalbumin-expressing interneurons linearly transform cortical responses to visual stimuli. *Neuron*, **73**, 159-170.

Bachatene, L., Bharmauria, V., Cattan, S. & Molotchnikoff, S. (2013) Fluoxetine and serotonin facilitate attractive-adaptation-induced orientation plasticity in adult cat visual cortex. *Eur J Neurosci*, **38**, 2065-2077.

Bachatene, L., Bharmauria, V., Cattan, S., Rouat, J. & Molotchnikoff, S. (2015) Reprogramming of orientation columns in visual cortex: a domino effect. *Sci Rep*, **5**, 9436.

Bachatene, L., Bharmauria, V. & Molotchnikoff, S. (2012a) Adaptation and Neuronal Network in Visual Cortex.

Bachatene, L., Bharmauria, V., Rouat, J. & Molotchnikoff, S. (2012b) Adaptation-induced plasticity and spike waveforms in cat visual cortex. *Neuroreport*, **23**, 88-92.

Bar, M. (2004) Visual objects in context. *Nat Rev Neurosci*, **5**, 617-629.

Bardy, C., Huang, J.Y., Wang, C., FitzGibbon, T. & Dreher, B. (2006) 'Simplification' of responses of complex cells in cat striate cortex: suppressive surrounds and 'feedback' inactivation. *The Journal of physiology*, **574**, 731-750.

Barlow, H.B., Blakemore, C. & Pettigrew, J.D. (1967) The neural mechanism of binocular depth discrimination. *The Journal of physiology*, **193**, 327-342.

Bharmauria, V., Bachatene, L., Cattan, S., Brodeur, S., Chanauria, N., Rouat, J. & Molotchnikoff, S. (2016) Network-selectivity and stimulus-discrimination in the primary visual cortex: cell-assembly dynamics. *Eur J Neurosci*, **43**, 204-219.

Bharmauria, V., Bachatene, L., Cattan, S., Chanauria, N., Rouat, J. & Molotchnikoff, S. (2015) Stimulus-dependent augmented gamma oscillatory activity between the functionally connected cortical neurons in the primary visual cortex. *Eur J Neurosci*, **41**, 1587-1596.

Budinger, E., Heil, P., Hess, A. & Scheich, H. (2006) Multisensory processing via early cortical stages: Connections of the primary auditory cortical field with other sensory systems. *Neuroscience*, **143**, 1065-1083.

Chabot, N., Charbonneau, V., Laramee, M.E., Tremblay, R., Boire, D. & Bronchti, G. (2008) Subcortical auditory input to the primary visual cortex in anophthalmic mice. *Neuroscience letters*, **433**, 129-134.

Chanauria, N., Bharmauria, V., Bachatene, L., Cattan, S., Rouat, J. & Molotchnikoff, S. (2016) Comparative effects of adaptation on layers II-III and V-VI neurons in cat V1. *Eur J Neurosci*, **44**, 3094-3104.

Clavagnier, S., Falchier, A. & Kennedy, H. (2004) Long-distance feedback projections to area V1: implications for multisensory integration, spatial awareness, and visual consciousness. *Cogn Affect Behav Neurosci*, **4**, 117-126.

Denman, D.J. & Contreras, D. (2014) The structure of pairwise correlation in mouse primary visual cortex reveals functional organization in the absence of an orientation map. *Cereb Cortex*, **24**, 2707-2720.

Daniel, B. (2011) Mechanisms of Cross-Modal Refinement by Visual Experience. Doctoral dissertation, Harvard University.

Deneux, T., Kempfl, A. & Bathellier, B. (2018) Context-dependent signaling of coincident auditory and visual events in primary visual cortex. doi.org/10.1101/258970.

Doron, N.N., Ledoux, J.E. & Semple, M.N. (2002) Redefining the tonotopic core of rat auditory cortex: physiological evidence for a posterior field. *The Journal of comparative neurology*, **453**, 345-360.

Dragoi, V., Rivadulla, C. & Sur, M. (2001) Foci of orientation plasticity in visual cortex. *Nature*, **411**, 80-86.

Dragoi, V., Sharma, J. & Sur, M. (2000) Adaptation-induced plasticity of orientation tuning in adult visual cortex. *Neuron*, **28**, 287-298.

Falchier, A., Clavagnier, S., Barone, P. & Kennedy, H. (2002) Anatomical evidence of multimodal integration in primate striate cortex. *J Neurosci*, **22**, 5749-5759.

Foxe, J.J. & Schroeder, C.E. (2005) The case for feedforward multisensory convergence during early cortical processing. *Neuroreport*, **16**, 419-423.

Frenkel, M.Y., Sawtell, N.B., Diogo, A.C., Yoon, B., Neve, R.L. & Bear, M.F. (2006) Instructive effect of visual experience in mouse visual cortex. *Neuron*, **51**, 339-349.

Fries, P., Nikolic, D. & Singer, W. (2007) The gamma cycle. *Trends Neurosci*, **30**, 309-316.

Fritz, J., Shamma, S., Elhilali, M. & Klein, D. (2003) Rapid task-related plasticity of spectrotemporal receptive fields in primary auditory cortex. *Nat Neurosci*, **6**, 1216-1223.

Ghazanfar, A.A. & Schroeder, C.E. (2006) Is neocortex essentially multisensory? *Trends Cogn Sci*, **10**, 278-285.

Ghisovan, N., Nemri, A., Shumikhina, S. & Molotchnikoff, S. (2008) Visual cells remember earlier applied target: plasticity of orientation selectivity. *PLoS One*, **3**, e3689.

Ghisovan, N., Nemri, A., Shumikhina, S. & Molotchnikoff, S. (2009) Long adaptation reveals mostly attractive shifts of orientation tuning in cat primary visual cortex. *Neuroscience*, **164**, 1274-1283.

Gielen, S.C., Schmidt, R.A. & Van den Heuvel, P.J. (1983) On the nature of intersensory facilitation of reaction time. *Perception & psychophysics*, **34**, 161-168.

Henry, G.H., Bishop, P.O., Tupper, R.M. & Dreher, B. (1973) Orientation specificity and response variability of cells in the striate cortex. *Vision Res*, **13**, 1771-1779.

Hershenson, M. (1962) Reaction time as a measure of intersensory facilitation. *Journal of experimental psychology*, **63**, 289-293.

Ibrahim, L.A., Mesik, L., Ji, X.Y., Fang, Q., Li, H.F., Li, Y.T., Zingg, B., Zhang, L.I. & Tao, H.W. (2016) Cross-Modality Sharpening of Visual Cortical Processing through Layer-1-Mediated Inhibition and Disinhibition. *Neuron*, **89**, 1031-1045.

Iurilli, G., Ghezzi, D., Olcese, U., Lassi, G., Nazzaro, C., Tonini, R., Tucci, V., Benfenati, F. & Medini, P. (2012) Sound-driven synaptic inhibition in primary visual cortex. *Neuron*, **73**, 814-828.

- Izraeli, R., Koay, G., Lamish, M., Heicklen-Klein, A.J., Heffner, H.E., Heffner, R.S. & Wollberg, Z. (2002) Cross-modal neuroplasticity in neonatally enucleated hamsters: structure, electrophysiology and behaviour. *Eur J Neurosci*, **15**, 693-712.
- Kayser, C. & Logothetis, N.K. (2007) Do early sensory cortices integrate cross-modal information? *Brain Struct Funct*, **212**, 121-132.
- Kayser, C., Petkov, C.I., Augath, M. & Logothetis, N.K. (2005) Integration of touch and sound in auditory cortex. *Neuron*, **48**, 373-384.
- Kayser, C. & Remedios, R. (2012) Suppressive competition: how sounds may cheat sight. *Neuron*, **73**, 627-629.
- Keller, G.B., Bonhoeffer, T. & Hubener, M. (2012) Sensorimotor mismatch signals in primary visual cortex of the behaving mouse. *Neuron*, **74**, 809-815.
- Liao, D.S., Krahe, T.E., Prusky, G.T., Medina, A.E. & Ramoa, A.S. (2004) Recovery of cortical binocularity and orientation selectivity after the critical period for ocular dominance plasticity. *Journal of neurophysiology*, **92**, 2113-2121.
- Lutcke, H., Margolis, D.J. & Helmchen, F. (2013) Steady or changing? Long-term monitoring of neuronal population activity. *Trends Neurosci*, **36**, 375-384.
- Macaluso, E. & Driver, J. (2005) Multisensory spatial interactions: a window onto functional integration in the human brain. *Trends Neurosci*, **28**, 264-271.
- Maffei, L., Fiorentini, A. & Bisti, S. (1973) Neural correlate of perceptual adaptation to gratings. *Science*, **182**, 1036-1038.
- Meijer, G.T., Montijn, J.S., Pennartz, C.M.A. & Lansink, C.S. (2017) Audiovisual Modulation in Mouse Primary Visual Cortex Depends on Cross-Modal Stimulus Configuration and Congruency. *J Neurosci*, **37**, 8783-8796.
- Moore, B.D.t., Alitto, H.J. & Usrey, W.M. (2005) Orientation tuning, but not direction selectivity, is invariant to temporal frequency in primary visual cortex. *Journal of neurophysiology*, **94**, 1336-1345.
- Muckli, L., De Martino, F., Vizioli, L., Petro, L.S., Smith, F.W., Ugurbil, K., Goebel, R. & Yacoub, E. (2015) Contextual Feedback to Superficial Layers of V1. *Curr Biol*, **25**, 2690-2695.
- Muckli, L., Kohler, A., Kriegeskorte, N. & Singer, W. (2005) Primary visual cortex activity along the apparent-motion trace reflects illusory perception. *PLoS Biol*, **3**, e265.
- Muckli, L. & Petro, L.S. (2013) Network interactions: non-geniculate input to V1. *Curr Opin Neurobiol*, **23**, 195-201.
- Oliva, A. & Torralba, A. (2007) The role of context in object recognition. *Trends Cogn Sci*, **11**, 520-527.
- Petro, L.S., Paton, A.T. & Muckli, L. (2017) Contextual modulation of primary visual cortex by auditory signals. *Philos Trans R Soc Lond B Biol Sci*, **372**.

Petro, L.S., Smith, F.W., Schyns, P.G. & Muckli, L. (2013) Decoding face categories in diagnostic subregions of primary visual cortex. *Eur J Neurosci*, **37**, 1130-1139.

Piche, M., Chabot, N., Bronchti, G., Miceli, D., Lepore, F. & Guillemot, J.P. (2007) Auditory responses in the visual cortex of neonatally enucleated rats. *Neuroscience*, **145**, 1144-1156.

Pluta, S., Naka, A., Veit, J., Telian, G., Yao, L., Hakim, R., Taylor, D. & Adesnik, H. (2015) A direct translaminar inhibitory circuit tunes cortical output. *Nat Neurosci*, **18**, 1631-1640.

Poort, J., Khan, A.G., Pachitariu, M., Nemri, A., Orsolich, I., Krupic, J., Bauza, M., Sahani, M., Keller, G.B., Mrsic-Flogel, T.D. & Hofer, S.B. (2015) Learning Enhances Sensory and Multiple Non-sensory Representations in Primary Visual Cortex. *Neuron*, **86**, 1478-1490.

Ramoia, A.S., Mower, A.F., Liao, D. & Jafri, S.I. (2001) Suppression of cortical NMDA receptor function prevents development of orientation selectivity in the primary visual cortex. *J Neurosci*, **21**, 4299-4309.

Ringach, D.L., Shapley, R.M. & Hawken, M.J. (2002) Orientation selectivity in macaque V1: diversity and laminar dependence. *J Neurosci*, **22**, 5639-5651.

Rockland, K.S. & Ojima, H. (2003) Multisensory convergence in calcarine visual areas in macaque monkey. *Int J Psychophysiol*, **50**, 19-26.

Rockland, K.S. & Van Hoesen, G.W. (1994) Direct temporal-occipital feedback connections to striate cortex (V1) in the macaque monkey. *Cereb Cortex*, **4**, 300-313.

Schroeder, C.E. & Foxe, J.J. (2002) The timing and laminar profile of converging inputs to multisensory areas of the macaque neocortex. *Brain Res Cogn Brain Res*, **14**, 187-198.

Schroeder, C.E., Smiley, J., Fu, K.G., McGinnis, T., O'Connell, M.N. & Hackett, T.A. (2003) Anatomical mechanisms and functional implications of multisensory convergence in early cortical processing. *Int J Psychophysiol*, **50**, 5-17.

Shuler, M.G. & Bear, M.F. (2006) Reward timing in the primary visual cortex. *Science*, **311**, 1606-1609.

Stevenson, R.A., Wallace, M.T. & Altieri, N. (2014) The interaction between stimulus factors and cognitive factors during multisensory integration of audiovisual speech. *Front Psychol*, **5**, 352.

Ten Oever, S., van Atteveldt, N. & Sack, A.T. (2015) Increased Stimulus Expectancy Triggers Low-frequency Phase Reset during Restricted Vigilance. *J Cogn Neurosci*, **27**, 1811-1822.

van Atteveldt, N., Murray, M.M., Thut, G. & Schroeder, C.E. (2014) Multisensory integration: flexible use of general operations. *Neuron*, **81**, 1240-1253.

Vetter, P., Smith, F.W. & Muckli, L. (2014) Decoding sound and imagery content in early visual cortex. *Curr Biol*, **24**, 1256-1262.

Vogels, R. (1999) Categorization of complex visual images by rhesus monkeys. Part 2: single-cell study. *Eur J Neurosci*, **11**, 1239-1255.

Xu, N.L., Harnett, M.T., Williams, S.R., Huber, D., O'Connor, D.H., Svoboda, K. & Magee, J.C. (2012) Nonlinear dendritic integration of sensory and motor input during an active sensing task. *Nature*, **492**, 247-251.

Yates, D. (2012) Sensory systems: sounds like competition. *Nat Rev Neurosci*, **13**, 222-223.